Fabrication and Opto-Electronic Modeling of Down-Shifting Enhanced Photovoltaics

Jose Raul Montes-Bojorquez, Maria Fernanda Villa-Bracamonte and Arturo A. Ayon

*The University of Texas at San Antonio, San Antonio, Texas, 78249, USA.

ABSTRACT

We report the fabrication and spectroscopic ellipsometry characterization of layer-by-layer assembled quantum dot multilayered films and their influence in the power conversion efficiency of silicon solar cells. The experimental performance of the resulting structure that possess downshifting and antireflective capabilities is compared to the theoretical predictions obtained from transfer matrix and FDTD simulations. The incorporation of the downshifting films on the front surface of the solar cell triggered an increase of 29.5% in the short circuit current density which is responsible for an increase in efficiency from 11.31% to 14.26%. The external quantum efficiency of the solar cell reproduced by the proposed theoretical formalism shows an excellent agreement with the experimental data, supporting the validity of the model and allowing the opto-electronic model assisted design of optimized downshifting structures for photovoltaic applications.

Keywords: layer-by-layer, quantum dots, photovoltaics, downshifting, ellipsometry.

1 INTRODUCTION

A purely optical approach to increase the short wavelength response of a PV material is the modification of the incident spectrum by a luminescent down-shifting (LDS) layer capable to absorb a high energy photon; inefficiently absorbed by the PV material, and emit a photon at lower energy that can be absorbed by the underlying solar cell. In this regard, quantum dots (QDs) are known to comprise a number of favorable characteristics as down-shifting materials for PV applications, namely, broad absorption spectra, large Stokes shift, high photoluminescent quantum yield (PLQY) and tunable emission spectra [1].

In addition to the potential efficiency enhancement due to LDS effects, the introduction of a LDS layer on a solar cell presents additional interactions with light, resulting in extra loss mechanisms. Specifically, when the LDS layer is placed on the front surface, it modifies the reflectance of the solar cell, and as a consequence the thickness of the layer as well as its refractive index are key factors in the performance of the resulted PV structure. Moreover, to effectively utilize the LDS effects of the QDs, a high optical absorption of the LDS layer is required.

In this work we propose a hybrid quantum dot/solar cell configuration to improve the spectral response of a silicon solar cell, as well as an opto-electronical theoretical formalism that allows the modeling of solar cell's quantum efficiency. Finally, we discuss possible ways to improve the performance of the presented structure.

2 EXPERIMENTAL DETAIL

2.1 Sample Preparation

2 × 2 cm planar p^+-n-n^+ cells were fabricated from 600 μm n-type, <100> oriented, single crystalline silicon wafer according to the procedure described in [2]. The multilayered polyelectrolyte-QD films were fabricated using electrostatic LBL assembly combined with spin-coating, based on the alternate deposition of negatively charged QDs and a positively charged polyelectrolyte. For this purpose, thioglycolic acid capped cadmium telluride QDs were synthesized employing a hydrothermal synthesis method [3], and poly(diallyldimethylammonium chloride) (PDDA) was used as the cationic polyelectrolyte.

After cleaning the solar cells with acetone and isopropyl alcohol, the thin films were deposited at double spin parameter settings (500 rpm - 10 s and 3000 rpm - 50 s) in the following order: (i.) first a 2% PDDA solution was spin coated, (ii.) the cell was rinsed with deionized water to remove the residual PDDA and dried while spinning, (iii.) then the PDDA terminated surface was spin coated with an aqueous solution of CdTe QDs, (iv.) finally the excess of QDs were rinsed with deionized water and dried while spinning. The cycle was repeated to obtain the desired number of bilayers. The fabrication ends with a thermal treatment at 100°C for 5 min to dry the sample.

2.2 Characterization

The UV–Vis absorption spectra and the photoluminescent effects of QDs were recorded using an Ocean Optics Flame-S-UV-VIS spectrometer. Ellipsometry measurements were carried out employing a variable angle,

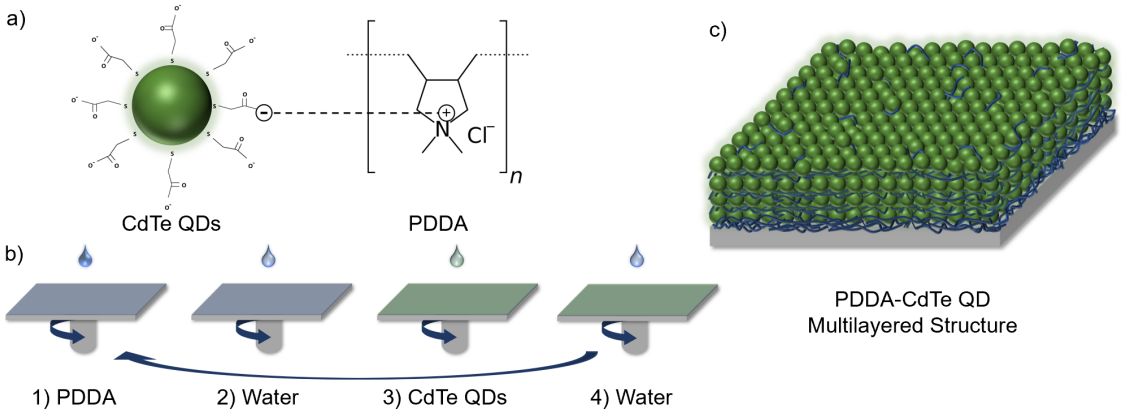

Figure 1: a) Schematic illustration of the electrostatic attraction between CdTe QDs and PDDA, (b) steps showing the process of fabricating PDDA-CdTe QD bilayers, (c) PDDA-CdTe QD composite on a silicon wafer.

rotating analyzer spectroscopic ellipsometer (Woollam Vase ellipsometer and WVASE software) in the wavelength range of 300 to 1100 nm. The current-voltage characteristic curves of the solar cells were measured using an Oriel Sol2A solar simulator under AM1.5G illumination. The external quantum efficiency (EQE) was measured with an Oriel Quantum Efficiency Measurement kit (QE-PV-SI).

3 RESULTS AND DISCUSSION

The PDDA adsorbed at the surface of the solar cells are positively charged under assembly conditions because of the numerous quaternary ammonium cations present on the polyelectrolyte chain [4], whereas TGA capped CdTe QDs contain negatively-charged carboxylate groups at the surface, making them good candidates for electrostatic LBL deposition (Fig. 1a). Traditional LBL deposition based on a repeated solution-dipping process was combined with conventional spin-coating to produce smother surfaces while reducing the processing time significantly. The process of film fabrication is accomplished through 4 steps illustrated in Fig. 1b. The resulting film allows high ordered close-packed structures and precise control of the thickness.

From the CdTe QDs synthesis, particles with a mean size of approximately 3 to 5 nm are obtained depending on the reflux time and the pH [3]. For an absorption spectra at $\lambda < 550$ nm and high PLQY, the time of the synthesis used in this work was set to 1 hour at a pH of 10.5. Fig. 2 shows the absorption and photoluminescence (PL) spectra of the synthesized QDs. The QDs have a 1s absorption peak at 519 nm which increases exponentially towards the ultraviolet (UV) part of the spectrum.

To obtain the thickness and optical constants (n and k) of the PDDA-QD film, an optical model was built using three Tauc-Lorentz oscillators. To measure each sample, a three layers model $Si/SiO_2/(PDDA\text{-}QDs)$ was used, where the thickness of the native SiO_2 was measured before the film deposition in each case and the parameters of the PDDA-QD optical model were fitted to the experimental ellipsometric spectra. Fig 3 shows the optical constants of the PDDA-QD film. The extintion coefficieny k resembles the shape of the colloidal QDs absorbance data, having a blue-shift of the first excitonic peak from 519 nm to 508 nm. In the case of a film, k also carries information about the structure and it can be used to calculate the absorption coefficient α and subsequently E_g [5]. It has been reported that the presence of nanoclusters at the surface leads to a decrease in the fundamental band gap of polyelectrolyte-QD LBL films [6], however, no significant changes were observed in the band gap of the LBL film in this work,

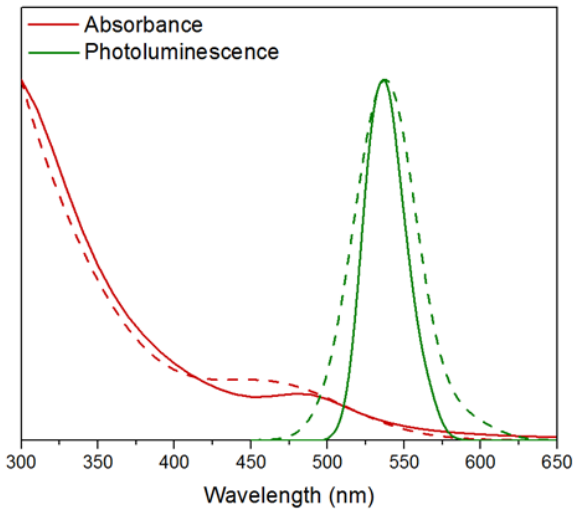

Figure 2: Absorption and PL of QDs in film (dashed line) and solution (continuous line).

TechConnect Briefs 2021, TechConnect.org, ISBN 978-0-578-99550-2

even when comparing the thickest film (3.51 eV) to the QDs in colloidal solution (3.55 eV). This supports the low surface roughness (∼3 nm) measured with ellipsometry.

Knowing the optical constants of the QD layer and the underlying films, the transfer matrix formalism can be used to model the reflection at the surface (R) of the solar cell after deposition of the LDS layer, as well as the parasitic absorption (A) of the QD layer and the transmission towards the active layer (T). To test the validity of the optical model, the intensity reflectance at near-normal incidence was measured for different number of PDDA-QD bilayers and compared to the modelled reflectance (Fig. 4). As the number of bilayers increases to 20 (37 nm) there is an increased optical coupling of light over a broad wavelength range, followed by a shift to longer wavelengths for thicker films, similar to the behavior of an antireflective coating (ARC) on a solar cell. This is a key factor explaining the observed increase in the external quantum efficiency (EQE) at long wavelengths where QDs do not absorb light, reported elsewhere [7].

Since the purpose of a LDS layer is to increase the short wavelength response of a solar cell, the influence of the LDS layer in the performance a solar cell can be evaluated by comparing the EQE before and after hybridization with QDs, however, in order to estimate the EQE response of the solar cell hybridized with QDs it is necessary to incorporate both, LDS and light coupling effects. If we assume that the LDS layer acts purely as an ARC, i.e., light is not re-emitted, the EQE after hybridization can be calculated as follows

$$EQE(\lambda) = IQE_{pn}(\lambda) \times T(\lambda), \quad (1)$$

where IQE_{pn} is the internal quantum efficiency of the solar cell before hybridization and it can be calculated from Eq.(1) in the absence of intermediate layers between the silicon/air interface, so that $T = 1 - R$.

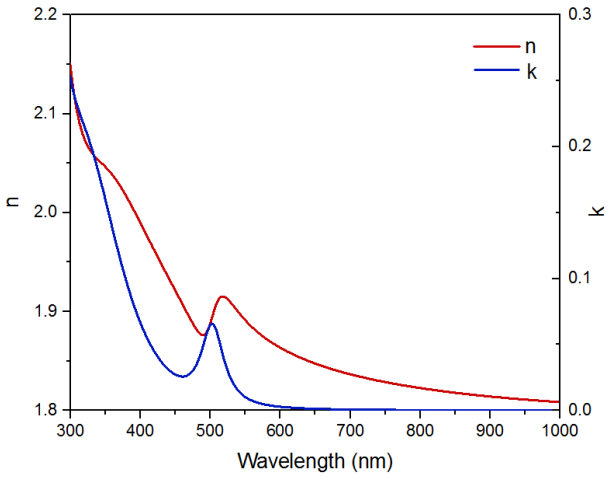

Figure 3: Optical constants of PDDA-QD film.

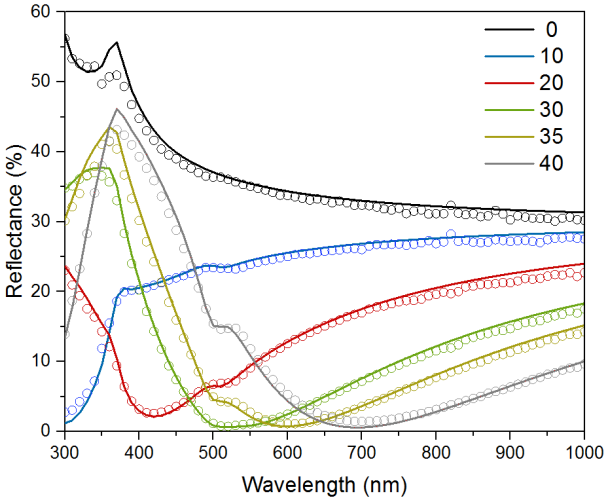

Figure 4: Modeled (continuous line) and measured (circles) reflectance of silicon solar cell for different number of PDDA-QD bilayers.

To analyze the influence of LDS on the performance of the solar cell, the photoluminescent spectra can be normalized as a probability distribution, so that $PL(\lambda)$ can be interpreted as the probability of a photon to be re-emitted at λ. Since not all the re-emitted photons reach the silicon surface, the probability of the down-shifted photon being re-emitted within the escape cone $P(\lambda)$ was calculated following the procedure of [8]. Finally, assuming no re-absorption losses, IQE_{pn} gives the probability of a re-emitted photon reaching the silicon surface to generate a charge carrier. Thus IQE_{LDS} defined as the ratio of the number of charge carriers collected by the solar cell to the number of photons of a given wavelength that are absorbed by the LDS layer is given by:

$$IQE_{LDS} = PLQY \times \int P(\lambda) IQE_{pn}(\lambda) PL(\lambda) d\lambda, \quad (2)$$

were the integral is over all the emission range.

It should be mentioned that if the quantum yield of the LDS layer is considered wavelength independent according to Kasha's rule [9], IQE_{LDS} is considered as well. Thus having to mechanisms for light absorption, the EQE of the hybridized solar cell is given by

$$EQE(\lambda) = IQE_{pn}(\lambda) \times T(\lambda) + IQE_{LDS}(\lambda) \times A(\lambda), \quad (3)$$

Notice that Eq.(3) implies that for a given λ the EQE of a solar cell remains unchanged if $IQE_{pn} = IQE_{LDS}$, thus a LDS will outperform an ideal ARC at those wavelengths where the internal quantum efficiency of a bare solar cell is less than IQE_{LDS}. Fig. 5 shows the measured EQE of a solar cell hybridized with different number of PDDA-QD bilayers (circles) compared to the model

using PLQY of 0.4 giving a IQE_{LDS} of 0.3 (continuous lines).

By maximizing the EQE response of the solar cell and thus the short circuit current density, an optimum thickness of 62 nm was found. To evaluate the performance of the PDDA-QD film in the power conversion efficiency, the current-voltage (I-V) characteristics of a solar cell were measured before and after the deposition of different PDDA-QD layer thicknesses (Fig. 6). Both, PCE and J_{sc} increase with the PDDA-QD layer thickness, reaching a maximum at around 35 bilayers (63.97 nm). This optimum device shows an enhancement in the PCE and J_{sc} of 26% and 29.5% respectively, compared to the bare solar cell. In adittion, the increase in thickness of the PDDA-QD film has little impact in the V_{oc} and field factor FF. The latter is consistent to an improvement in PCE fully driven by an increase in sunlight absorption rather than a change in the electrical properties of the cell.

Since the refractive index of QDs is known to be size dependent [10], a multilayered structure was modeled for which the thickness and refractive index were set as parameters to be optimized. Using a finite-difference time-domain (FDTD) model of Lumerical FDTD solutions 8.25.2621 and particle swarm optimization, it was found that by adding an additional film with average refractive index of 3 to the fabricated structure, the average reflectance is reduced from 5.85% to 2.63%, while the optimum total thickness is increased to 138 nm and thus increasing the QD load.

4 CONCLUSIONS

In this work a luminescent downshifting multilayered film was fabricated via the electrostatic LBL assembly to boost the spectral response of a solar cell. Based on the spectroscopy ellipsometry characterization of the multilayered films, an analytical model of the external quantum efficiency was developed, which demonstrated an excellent agreement with the experimental performance of the proposed nanostructures. For the optimum thickness, an improve in the power conversion efficiency from 11.31% to 14.26% was found, fully driven by an increase in the short circuit current density from 30.75% to 39.84%.

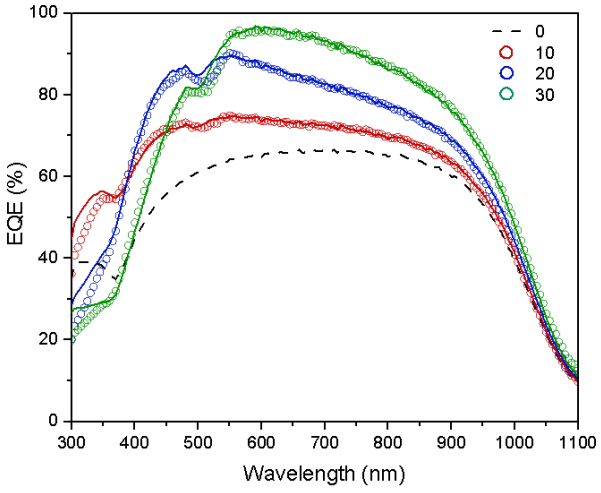

Figure 5: EQE of solar cells with different number of PDDA-QD films.

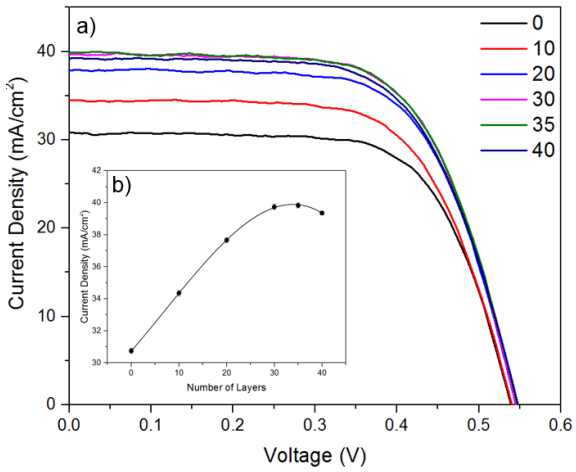

Figure 6: a) J-V curves and (b) short circuit current density (J_{sc}) of silicon solar cell before and after the deposition of different thicknesses of PDDA-QD films.

REFERENCES

[1] A. Flores-Pacheco, M. Alvarez-Ramos, and A. Ayon, Elsevier, 2020, pp. 443–477.

[2] R. Montes and A. Ayon, presented at the 48th IEEE PVSC, 2021.

[3] S. Wu, J. Dou, J. Zhang, and S. Zhang, J. Mater. Chem. , vol. 29, pp. 5998–6009, 2012.

[4] D. Kumar, B. Kumar, and H. Mahesh, J. Alloys Comp., 735, pp. 2558–2566, 2018.

[5] J. Tauc, J. Mat. Res. Bull, vol. 3, pp. 37–46, 1968.

[6] E. Lioudakis, E. Koupanou, C. Kanari, E. Leontidis, and A. Othonos, J. Appl. Phys., vol. 103, pp. 083511, 2008.

[7] C. Krishnan, T. Mercier, T. Rahman, G. Piana, M. Brossard, and M. Charlton, Nanoscale, vol. 11, pp. 18837–18844, 2019.

[8] W. Shurcliff and C. Jones, J. Opt. Soc. Am., vol. 39, pp. 912–916, 1949.

[9] M. Kasha, Discussions of the Faraday Society, vol. 9, pp. 14–19, 1950.

[10] F. Mezraga and N. Bouarissa, Mat. Res., vol. 22, 2019.